Published in final edited form as:
Cell. 2012 January 20; 148(1-2): 164–174. doi:10.1016/j.cell.2011.11.023.

Requirements for Efficient Correction of ΔF508 CFTR Revealed by Analyses of Evolved Sequences

Juan L. Mendoza[1,2], **André Schmidt**[2], **Qin Li**[3], **Emmanuel Caspa**[2], **Tyler Barrett**[2], **Robert J. Bridges**[5], **Andrew P. Feranchak**[3], **Chad A. Brautigam**[4], and **Philip J. Thomas**[1,2,*]

[1]Molecular Biophysics Program, University of Texas Southwestern Medical Center, Dallas, Texas 75390-9040

[2]Department of Physiology, University of Texas Southwestern Medical Center, Dallas, Texas 75390-9040

[3]Department of Pediatrics, University of Texas Southwestern Medical Center, Dallas, Texas 75390-9040

[4]Department of Biochemistry, University of Texas Southwestern Medical Center, Dallas, Texas 75390-9040

[5]Department of Physiology and Biophysics, Rosalind Franklin University, Chicago, Illinois 60064

SUMMARY

Misfolding of ΔF508 CFTR underlies pathology in most CF patients. F508 resides in the first nucleotide binding domain (NBD1) of CFTR near a predicted interface with the fourth intracellular loop (ICL4). Efforts to identify small molecules that restore function by correcting the folding defect have revealed an apparent efficacy ceiling. To understand the mechanistic basis of this obstacle, positions statistically coupled to 508, in evolved sequences, were identified and assessed for their impact on both NBD1 and CFTR folding. The results indicate that both NBD1 folding and interaction with ICL4 are altered by the ΔF508 mutation and that correction of either individual process is only partially effective. By contrast, combination of mutations that counteract both defects restores ΔF508 maturation and function to wild type levels. These results provide a mechanistic rationale for the limited efficacy of extant corrector compounds and suggest approaches for identifying compounds that correct both defective steps.

INTRODUCTION

Cystic fibrosis (CF) is a lethal, monogenic disease caused by dysfunction of the Cystic Fibrosis Transmembrane Conductance Regulator (CFTR). CFTR is a member of the ATP-Binding Cassette (ABC) transporter family that functions as a chloride channel. The protein is composed of five domains: two transmembrane domains (TMDs) which form the channel through the membrane, two nucleotide binding domains (NBDs) which gate the channel through ATP binding and hydrolysis reactions, and a regulatory region (R) which mediates kinase-dependent regulation of activity (Figures 1A–B) (Berger et al., 2005; McCarty, 2000;

*Correspondence: Philip J. Thomas, philip.thomas@utsouthwestern.edu, Department of Physiology, UT Southwestern, 6001 Forest Park, Dallas, TX 75390-9040 telephone: (214) 645 6009.

Mendoza and Thomas, 2007; Riordan et al., 1989; Vergani et al., 2005). Most commonly, CF is associated with the deletion of a single amino acid, Phe 508, in the first NBD (NBD1) of CFTR (Figures 1A–C) (Riordan et al., 1989). ΔF508 CFTR fails to fold properly and does not efficiently traffic to the plasma membrane (Cheng et al., 1990) resulting in a loss-of-function (Rich et al., 1990). The mutant CFTR is active when induced to fold and traffic to the membrane (Denning et al., 1992; Teem et al., 1993) indicating that compounds that correct the folding defect may have therapeutic benefit.

Studies of the NBD1 of CFTR indicate that the deletion reduces folding efficiency (Qu and Thomas, 1996; Thibodeau et al., 2005) and stability (Hoelen et al., 2010; Protasevich et al., 2010; Thibodeau et al., 2010; Thomas et al., 1992; Wang et al., 2010). Crystal structures of the isolated CFTR-NBD1 domains reveal that F508 is partially exposed on the surface (Lewis et al., 2004) and that deletion of the residue causes only local rearrangements in the loop following the 508 residue in the context of stabilizing mutations that facilitated crystallization (Atwell et al., 2010; Lewis et al., 2005).

Evidence suggests that ΔF508 CFTR can be targeted to improve folding and restore function. A patient with a less severe form of CF had ΔF508-R553Q on one allele and a nonsense mutation on the other (Dork et al., 1991). A mating-screen in yeast utilizing a CFTR - Ste6 chimera identified the same R553Q mutation as a suppressor of the loss-of-mating ΔF508 phenotype (Teem et al., 1993). Additional second-site revertant mutations I539T, G550E, R553M, and R555K, within the portion of CFTR NBD1 included in the chimera, were also identified (DeCarvalho et al., 2002; Teem et al., 1993; Teem et al., 1996). The R553M, I539T and the combination of G550E-R553M-R555K (3M) mutations correct the folding and stability defects of the ΔF508 NBD1 domain in isolation (DeCarvalho et al., 2002; Hoelen et al., 2010; Pissarra et al., 2008; Qu et al., 1997; Thibodeau et al., 2010), but only partially restore maturation of the full-length mutant protein (Hoelen et al., 2010; Pissarra et al., 2008; Thibodeau et al., 2010). These data indicate that correction of the NBD1 folding defect alone only incompletely restores maturation of ΔF508 CFTR.

Based on the hypothesis that compounds that effectively improve the folding of ΔF508 CFTR would be of therapeutic benefit, several cell-based high-throughput screens have been performed (Pedemonte et al., 2005; Robert et al., 2010; Robert et al., 2008; Van Goor et al., 2006). While some of the compounds identified bind to and stabilize NBD1 (Sampson et al., 2011); the mechanism of action of most remains unknown. None of the reported ΔF508 correctors have potency much less than 1 μM and, like the single intragenic second site-suppressor mutants, efficacy above about 15% of wild type levels (Van Goor et al., 2011). There is reasonable concern that this degree of correction will not provide therapeutic benefit based on the promising results with the more potent and efficacious potentiator of the rarer CF-causing G551D gating mutant (Accurso et al., 2010; Van Goor et al., 2009). This potentiator compound, VX-770, demonstrates that pharmacological improvement of mutant CFTR function in adult patients provides a measurable clinical benefit (Accurso et al., 2010), further stimulating the search for effective correctors of ΔF508 folding and function. Understanding the molecular basis of the apparent correction ceiling and the mechanism of action of corrector compounds would provide critical insight for development of corrector compounds.

The identification of positions coupled to F508, provided by the Ste6-CFTR chimera revertant mating screen, has provided insights into CFTR folding and the effect of ΔF508, but was limited to residues immediately proximal to the F508 position (Teem et al., 1993; Teem et al., 1996). Extending such a second-site analysis to the whole of CFTR might be expected to provide new information about the folding and maturation of CFTR and the

effect of the ΔF508 mutation thereon—information critical for revealing the mechanism of action of extant correctors, for developing methods capable of identifying better compounds, and for a fundamental understanding of the process of membrane protein folding. In the absence of a conveniently assessed phenotype for CFTR function as required to evaluate millions of individual genetic perturbations, the information nature has provided in the sequences of the ABC supergene family offer an alternative. Multiple algorithms have been developed that can identify residues coupled to specific positions, for example F508, in the evolved sequences of protein homologues (Fodor and Aldrich, 2004; Goh et al., 2000; Kass and Horovitz, 2002; Lockless and Ranganathan, 1999; Pazos and Valencia, 2008; Socolich et al., 2005). The set of residues statistically coupled to the F508 position would be expected to be enriched for positions that interact directly or allosterically in the final structures or transiently during the process of folding. Such interactions should be evident in the stability and folding yield of NBD1 and the maturation of CFTR, which reflects the association of folded NBD1 with ICL4. In the present work we identified positions coupled to F508 in CFTR and determined their effect on both NBD1 folding and CFTR maturation. The results reveal the quantitative effect of the ΔF508 mutation on two distinct steps of folding and, further, suggest mechanistically defined methodologies for identifying compounds targeting either or both steps defective in the mutant protein.

RESULTS

Positions Coupled to 508 in the ABC Transporter Supergene Family

CFTR is a member of the ABC transporter supergene family (Dean and Annilo, 2005). Over 2,000 full-length sequences of eukaryotic ABC Transporters (containing two NBDs and two TMDs on a single polypeptide) were obtained from iterations of a PSI-Blast default search using the human CFTR protein sequence as the seed (gi 90421313). Four multiple sequence alignments (MSA) were generated using ClustalW (Larkin et al., 2007). After quality assessment using the three highly conserved Walker A and B, and Consensus motifs (Dean and Allikmets, 1995; Dean and Annilo, 2005; Jones and George, 2004; Walker et al., 1982), the sequences to be queried was reduced by half. Removal of additional sequences that had greater than 90% identity to any other sequence, produced a set of 493 full-length sequences (MSA available for download at http://cftrfolding.org). The NBD domains have the highest number of conserved positions in the MSA. Four positions in CFTR are invariant in the alignment, K464 and G1244 in the Walker A motifs of NBD1 and NBD2, respectively, Q1292, the Q-loop residue in NBD2, and D1370 of the NBD2 Walker B motif. The TMDs have high conservation at or near the ICLs. The scores in the R-domain approach randomness (conservation score of −1). Phe is the most common amino acid at the 508 position followed by Tyr at frequencies of 0.86 and 0.11, respectively.

Matrices of the pairwise correlation scores were calculated using the MSA by four independent, statistical methods; Statistical Coupling Analysis (SCA), Explicit Likelihood of Co-variation (ELSC), OMES, and McBASC (Figures 2A–B, and S2) (CSV files are available for download at http://cftrfolding.org) (Dekker et al., 2004; Fodor and Aldrich, 2004; Lockless and Ranganathan, 1999). The top 20 statistical 508-coupled positions for the four methods formed a set of 45 positions (Table 1). A random set of 16 of these 45 508-coupled positions (Table 1 and Figure S3), were assessed for effects on CFTR folding. The 16 positions represent ~78% coverage of the top ten 508-coupled positions for all four methods, and include 6 positions common between all 4 methods, 2 positions between 3 methods, 6 positions between 2 methods, and 2 positions unique to a single method (Table 1). The 6 coupled positions common between all 4 methods are located in the α-helical subdomain (Table 1 and Figure S3). Ten of the 16 positions are surface exposed; F490L and W496, like F508, are predicted to be at the ICL4 interface (Table 1 and Figure S3). Additional positions reside within the coupling helix boundaries of ICL1 and ICL4 (Figure

2B). Each of the 16 positions in CFTR was mutated to the most common non-CFTR amino acid (Table 1) and the effect on both NBD1 folding and CFTR maturation was assessed.

Mutations at 508-Coupled Positions Effect NBD1 Folding

The 16 508-coupled positions and previously identified second-site suppressor mutations, and combinations thereof, were evaluated for effects on the folding of the isolated human CFTR NBD1 using a structural complementation assay described (Thibodeau et al., 2010; Wigley et al., 2001). In the current implementation of the assay, the folding signal of ΔF508 NBD1 was 0.43 ± 0.03 relative to wild type NBD1, 1.00 ± 0.03. All 16 508-coupled and second-site suppressor mutations had a significant effect on the folding of the isolated domain relative to wild type (Figure 3A) suggesting the statistical analyses identified a set enriched for biological relevance. Fourteen of the 508-coupled mutations interfered with NBD1 folding (Figure 3A, green bars). The significance of the decrease in folding was less than $6E^{-6}$ for 13 of the mutants and 0.002 for the least significant, E583G. Two 508-coupled mutants, D529F and S573E, dramatically increased the relative folding yield of NBD1 by 3.07 ± 0.13 and 1.85 ± 0.06 fold, respectively, a level comparable to that of the second-site suppressors identified in the STE6 chimera screen (Figure 3A).

Thermal denaturation of purified D529F and S573E NBD1 revealed that S573E raised the T_m by 2–5 °C relative to wild type depending on ATP concentration (Figure S4B), indicating the improved folding yield in the complementation assay could be accounted for by increased stability of the native state (Figure 3B). In stark contrast, D529F had no measureable effect on T_m indicating the complementation assay reflects changes in yield and pathway as well as changes in stability or solubility. D529 is located in the α-helical sub-domain of NBD1 near the NBD1/NBD2 interface (Figure 1C). Analysis of the human NBD1 crystal structures (pdb 2BBO and 1XMI) reveals this aspartic acid side chain forms a salt bridge with R555. The R555 side chain also makes a hydrogen bond with the backbone carbonyl of Q525 (Figure S4A). The R555K missense mutation is one of the previously studied second-site suppressors of ΔF508 NBD1 mediated misfolding (Roxo-Rosa et al., 2006; Teem et al., 1996). R555K increased the folding yield of NBD1, 3.26 ± 0.07 fold over wild type (Figure 3A). The T_m of R555K NBD1 was 6.4 °C higher than wild type in 2 mM ATP. A Glu or Asp at the CFTR equivalent 573 position is the catalytic base in the highly conserved Walker B motif in other ABC Transporters (Jones and George, 2004; Mendoza and Thomas, 2007; Walker et al., 1982). The serine present in CFTR at this position accounts for the lack of ATP hydrolysis at this site as central to the mechanochemistry of the gating cycle (Figure S4B) (Vergani et al., 2003).

Mutations at 508-Coupled Positions Effect Maturation

To examine the relationship of NBD1 folding and stability with full-length CFTR folding, mutant CFTRs were expressed in HeLa cells and CFTR maturation was determined by two methods. As CFTR folds, it traffics from the ER to the Golgi where it attains complex glycosylation prior to reaching the plasma membrane. The resulting increase in molecular mass can be detected by western blotting of SDS-PAGE (Figure 4). The slower migrating complex glycosylated Band C reflects the folded, mature CFTR while the more rapidly migrating Band B reflects core glycosylated CFTR that has not reached the Golgi (Cheng et al., 1990). This data has been utilized in several ways to monitor the effect of mutations and compounds on CFTR folding. The ratio of Band C to Band B is linear with both CFTR at the surface as monitored by biotinylation and with Band C itself (Figure S5C). By contrast the ratio of Band C over total CFTR has a nonlinear relationship with mature surface CFTR, being more sensitive to changes at low folding yields (Figure S5B). In these analyses it was noted that none of the mutants tested had a significant effect on the amount of Band B and thus, the total CFTR was linear with the amount at the surface (Figure S5C). An ELISA

assay for total CFTR quantitation was developed and used to monitor CFTR maturation. The signal from this method is not only linear but has lower noise than other methods (Figure S5C). The influence of all the 508-coupled mutants on CFTR folding was assessed (Figure 4A). All sixteen of the 508-coupled mutations and second-site suppressor mutations altered the yield of full-length CFTR relative to wild type. The same 14 mutations that reduced the yield of NBD1 folding, reduced maturation of full-length CFTR (Figure 4A, green bars). The P-value for all is less than 0.04. The same two mutations that improved NBD1 folding yield, D529F and S573E, increased the maturation efficiency of CFTR (Figure 4A, yellow and magenta bars, respectively). The previously identified second-site suppressor mutants also improved CFTR maturation in a manner consistent with their effects on NBD1 folding. The correlation between NBD1 folding and CFTR maturation is formalized in Figure 4B. The data indicate a linear relationship (R = 0.85) with a slope of 0.75. Thus, NBD1 folding is necessary for CFTR folding and for every fold change in NBD1 yield a concomitant change of 0.75 in CFTR yield is observed. The position along the x axis thus reflects the amount of folded NBD1 and the slope of the line likely reflects later steps in folding during which folded NBD1 associates with other parts of CFTR.

Influence of ΔF508 on NBD1 Folding and Later Steps in CFTR Maturation

To determine whether in addition to its known effects on NBD1 folding and stability, ΔF508 interferes with later steps in CFTR folding, the differential effects of the NBD1 suppressor mutations on the wild type and ΔF508 NBD1 folding yield and CFTR maturation yield were measured and correlated (Figure 5B). Interestingly, the two suppressors identified by the coupling analysis, D529F and S573E, had much more modest effects on NBD1 yield in the presence of the ΔF508 mutant as might be expected. Taken together, the suppressors define a line (m = 0.10, R = 0.36) in the context of ΔF508 indicating the mutation interferes with a later step in CFTR folding in addition to its defect in NBD1 folding yield. Thus, the mutation decreases NBD1 folding yield approximately three fold and later CFTR folding steps by approximately seven fold.

Extant structures of CFTR ΔF508 NBD1 contain a series of previously identified second-site mutations that improve folding and solubility of the model domain. To simplify structural interpretation of the current results, a high resolution structure of murine ΔF508 NBD1 without additional mutations or deletions was solved (Table S1). Comparison of the backbones of the murine wild type (pdb 1R0W) and ΔF508 NBD1 (pdb 3SI7) structures reveal nearly identical structures, RMS 0.249 Å, with backbone shifts immediately following the 508 position. The largest shift in C_α between the two structures is G509 shifting by 3.5 Å followed by a 1.5 Å shift for V510 before the Δ F508 backbone converges with wild type. The surface view of the two structures suggests local changes near the site of the deletion (Figure S1) similar to the structures containing the second-site mutations (Lewis et al., 2010; Lewis et al., 2005). The absence of the F508 side chain creates a significant pocket on the surface of NBD1 at the predicted interface between ICL4 and NBD1 (Figure S1B). Additionally, the V510 side chain rotates outwardly 3.6 Å (C_β) from the core in the mutant structure, further increasing the size of the pocket.

To better understand the molecular basis of the later step in folding effected by the ΔF508 mutation, we built upon earlier work indicating that most missense mutations at the 508 position do not have dramatic effects on NBD1 but rather interfere with CFTR maturation (Du et al., 2005; Thibodeau et al., 2005). The current assay battery was applied to a set of these mutations alone or in combination with the NBD1 suppressors (Figure 5C). When F508 is replaced by Lys very little CFTR maturation is observed regardless of the ability of the NBD1 to fold (m = 0.03, R = 0.38). The model of CFTR (Mendoza and Thomas, 2007) based on alignment with Sav1866 (Dawson and Locher, 2007) places F508 (or the ΔF508 pocket) near R1070 in ICL4 (I218 in ICL2 of Sav1866) (Figure 5C, *top*). Residues in ICL4

coupled to the 508 position exhibit a helical pattern consistent with the structural model. To assess the NBD1 - ICL4 interface from the ICL4 side of the interface, a large tryptophan side chain replaced the native arginine. The R1070W sterically clashes with the F508 position in the model (Figure 6A, *top*) a prediction consistent with fact that it is a CF-causing mutation (Krasnov et al., 2008) that inhibits CFTR maturation when F508 is present (open circle, Figure 6A, *bottom*). By contrast, the introduction of the larger side chain at 1070 is accommodated by the ΔF508 pocket in the mutant NBD1, and, could allow for better packing (Figure 6B, *top*) that promotes folding (open triangle, Figure 6A, *bottom*) by correcting the ICl4 - ΔF508 NBD1 interface defect.

The ability of the R1070W mutation to counteract the ICL4 - NBD1 interface defect caused by the ΔF508 mutation, allowed assessment of the quantitative effects of suppression of both defects concurrently. When NBD1 suppressor mutations were introduced on top of R1070W and ΔF508, the slope was restored (m = 0.77, R = 0.47) (Figure 6B). Thus, correction of the two defects results in near total rescue of the mutant folding phenotype. A three-fold improvement in ΔF508 NBD1 folding yield, correcting the NBD1 to wild type levels, results in a modest improvement in CFTR maturation (0.10 slope). Similarly, the R1070W interface mutant produces an approximately seven fold increase in the slope, but only a modest improvement in CFTR maturation. However, when the two effects are combined, they have a multiplicative effect on folding.

CF is a loss-of-function disease. To determine if efficient correction of maturation was adequate to restore function, CFTR activity was measured for mutations that corrected either the NBD1 defect or the ICl4/NBD1 defect or both. Two assayed were employed: transepithelial ion conductance was determined in FRT cell monolayers (Figure 6C) and whole cell currents were measured in HeLa cells (Figure 6D). CFTR dependent function was taken as the forskolin dependent, inh-172 sensitive activity. Mirroring the maturation results, correction of either the NBD1 defect (I539T, R555K, red bars) or the ICL4/NBD1 defect (R1070W, white bar) alone provided only modest improvements of function. Like maturation, combination of the two types of correction mutations (cyan bars) had a synergystic effect, restoring CFTR function to near wild type levels.

DISCUSSION

The most common cystic fibrosis causing mutation, ΔF508, disrupts the normal folding pathway of CFTR leading to the loss-of-function that underlies pathogenesis (Cheng et al., 1990). The mutant protein is active when induced to fold (Denning et al., 1992; Teem et al., 1993) suggesting a novel pharmacological approach to treating CF. Small molecules that bind to and counteract the folding ΔF508 defect would provide a means of repairing the protein (Thomas et al., 1992) while maintaining normal regulation and expression patterns. Multiple efforts to identify such compounds have been reported (Pedemonte et al., 2005; Robert et al., 2010; Robert et al., 2008; Sampson et al., 2011; Van Goor et al., 2006), but the identified molecules are not very potent and correct mutant CFTR folding to no more than 15% of wild type (Van Goor et al., 2011). Understanding the basis of this observed efficacy ceiling would provide information critical for determining the feasibility of the corrector approach and guide any future discovery efforts. Although it is known that CFTR folding is a hierarchical process that occurs partially during translation (Du et al., 2005; Hoelen et al., 2010; Thibodeau et al., 2005) and that the ΔF508 mutation interferes with NBD1 folding (Hoelen et al., 2010; Protasevich et al., 2010; Thibodeau et al., 2005; Thomas et al., 1992) and is reflected in other domains (Du et al., 2005), fundamental details of the folding pathway and its disruption are lacking.

To gain insight, we identified residues coupled to the 508 position utilizing a computational approach. Several methods have been developed to use evolutionary sequence analysis to identify networks of residues within proteins important for function, to improve native intermolecular contact prediction algorithms, and to identify hot spots of ligand binding or protein-protein interactions (Dekker et al., 2004; Goh et al., 2000; Lockless and Ranganathan, 1999; Madaoui and Guerois, 2008; Pazos and Valencia, 2008; Socolich et al., 2005). We used the ABC transporter family to identify positions related to F508 and its important role in folding. Multiple evolutionary coupling algorithms were utilized to identify relevant positions. Remarkably, the 16 508-coupled mutants selected and tested all effect the folding of both the isolated domain and the full-length CFTR. Fourteen mutations made folding worse and two improved the folding. These results are not likely to occur by random chance. For example, two random mutant screens found 0.03% of clones in the library improved folding, while, 20% of mutants misfolded with an average of two mutations per clone, demonstrating the inherent mutational robustness of proteins (Kunichika et al., 2002; Pjura et al., 1993) and the utility of the computational methods. In comparison to the random screens, we were 400 times more likely to identify mutations which improve folding and 4 times more likely to identify mutations which result in misfolding.

Identified in this study, D529F and S573E improve folding of NBD1 in isolation and maturation of full-length CFTR in the wild type background. The human CFTR 573 position corresponds to a highly conserved Glu, the catalytic base, of the Walker B motif in other members of the ABC transporter family and in the second NBD of CFTR (Walker et al., 1982). However, CFTR proteins have a serine at this position, accounting for the lack of ATPase activity at this site. Reversion to Glu does not restore catalytic activity at this site indicating there are other changes important in the evolution of CFTR as a channel from a family of transporters (Stratford et al., 2007; Vergani et al., 2003). In this work, we found the wild type protein is less stable than the mutant containing the conserved residue (Figures 3B, leftmost panel, and S4B).

Analyses of identified coupled positions in the wild type and ΔF508 backgrounds, utilizing methodologies to facilitate the large number of samples, demonstrated that there are two steps in CFTR folding in which ΔF508 is defective; NBD1 folding and a later step involving NBD1 and ICL4. The correction of only one defect by suppressor mutations or compounds has limited efficacy as is reflected in the partial maturation and function of ΔF508 CFTR to less than 20% of wild type, the previously observed “ceiling”. In plots of CFTR folding yield against NBD1 folding yield, the position along the x axis reflects the first step in folding and the slope of the line reflects the later steps including the NBD1/ICL4 interface.

The experiments with the second-site suppressor mutations on the F508K background demonstrate, regardless of how well NBD1 folds, CFTR is unable to mature if the NBD1/ICL4 is disrupted; likewise, CFTR cannot mature if NBD1 is unable to form a native structure. These findings predict that screens for compounds that improve CFTR maturation or function might be biased against compounds that act specifically against either individual folding defect as they would produce improved position on the x axis or a steeper slope, but little actual improvement of CFTR maturation and function. Unless single compounds can correct both steps, the set of highest hits in such screens are likely to be populated with compounds that do not directly act on CFTR. Thus, these findings have implications for the discovery and development of CF therapeutics. Compounds, or combinations of compounds, that correct both defective steps could provide both on target specificity and efficacy of action. The assay systems and second-site mutants developed may also find utility in establishing a mechanism of action of extant correctors and aid in the identification of new compounds.

EXPERIMENTAL PROCEDURES

Bioinformatics

The human CFTR sequence (gi|90421313) was used as a seed for PSI-Blast (Altschul et al., 1997) of the non-redundant database. Sub-alignments were performed using ClustalW and assessed (Larkin et al., 2007). Sequences lacking conserved ABC Transporter motifs (Walker A, B, and/or Consensus motifs) (Walker et al., 1982) were removed. The final alignment was generated online using Promals 3D (Pei et al., 2008a; Pei et al., 2008b). Proteins >90% identity to any other protein in the alignment were removed. The alignment contains 493 sequences. Positional entropy based conservation scores were calculated using AL2CO (Pei and Grishin, 2001) and frequencies of the most common amino acid position identified and calculated via Perl scripting.

The multiple sequence alignment was used to calculate pairwise correlation matrices using Statistical Coupling Analysis (Lockless and Ranganathan, 1999), Explicit Likelihood Subset of Co-variation (Dekker et al., 2004), OMES (Kass and Horovitz, 2002; Larson et al., 2000) (Fodor and Aldrich, 2004; Kass and Horovitz, 2002), and McBASC (Gobel et al., 1994; Olmea et al., 1999). Pairwise correlation scores for SCA were calculated in Matlab (The MathWorks Inc.) using the algorithm provided by Ranganathan. ELSC, OMES, and McBASC scores were calculated using the downloaded package from A. Fodor (afodor.net). Mutations at each of the positions were selected utilizing amino acid distribution profiles complementing correlated changes at the 508 position.

NBD1 Folding Yield

pcDNA 3.1(+) constructs containing human WT and ΔF508 CFTR NBD1 (residues 389-673) were used as previously described (Thibodeau et al., 2010; Wigley et al., 2001). HeLa TetOn (Clontech Laboratories Inc.) cells were transiently transfected using Lipofectamine 2000 (Invitrogen Corp.) at a cell density of 320,000 cells/ml. After transfection, cells were grown at 37°C for 18–24 hours. Media was aspirated from each well and 50 λ of 2.5 μM fluorescein-di-β-D-galactopyranoside (FDG) (Sigma-Aldrich Corp.) substrate in Reporter lysis buffer (Promega Corp.) added. Fluorescence was measured every minute for 24 hours. Rates were determined from the linear portions of the data. P-values were determined using the Student's T-test with a two-tail distribution of a two-sample heteroscedastic test.

CFTR Maturation Yield

With pCMV-CFTR (a gift from J. Rommens) HeLa TetOn (Clontech) cells were transiently transfected with Lipofectamine 2000 (Invitrogen) and grown at 37°C for 24 hours. Effects of mutations on maturation of CFTR was visualized by western blot analysis and quantitated by a sandwich ELISA utilizing mAb A596 (J. Riordan, UNC) as the capture antibody and 3G11 (W. Balch, Scripps) as the detection antibody. Characterization of the ELISA maturation assay and detailed methods are included in the Extended Experimental Procedures and Figure S5.

Protein Expression, Purification, and Characterization

Murine ΔF508 NBD1, 389-673 human numbering, was expressed and purified as previously described except bacterial pellets were not frozen (Lewis et al., 2004). D529F, S573E, and R555K mutations of human wild type NBD1 were expressed and purified as previously described (Thibodeau et al., 2005). Temperature melts were performed at 2 mM ATP (Hoelen et al., 2010).

ΔF508 NBD1 Crystallization and Structure Determination

Crystals of murine CFTR NBD1 ΔF508 were grown using the vapor-diffusion method by mixing 1 μL of 10 mg/ml of the murine ΔF508 NBD1 protein with 1 μL of the well solution (containing 3.5–4 M sodium acetate, pH 7.5) (Lewis et al., 2004; Thibodeau et al., 2005). Crystals used for data collection were flash-cooled by suspending in a nylon loop directly out of their mother liquor and then plunging into liquid propane. X-ray diffraction data were acquired at beamline 19-ID at the Structural Biology Center of the Advanced Photon Source at Argonne National Laboratories. Statistical details of the final model are found in Table S1.

Homology Model of CFTR

Murine NBD1 or ΔF508 (pdb 1R0W or 3SI7) and human NBD2 (pdb 3GD7) were docked onto the Sav1866 structure (pdb 2HYD) (Dawson and Locher, 2007; Lewis et al., 2004). A set of sequences containing the ICL4 segments of CFTR proteins and Sav1866 ICL2 was used to generate an alignment using the JalView ClustalW function (Clamp et al., 2004; Waterhouse et al., 2009). On the WT or ΔF508 CFTR models, F508K, R1070, R1070W residues were modeled using the Pymol (Schrodinger, 2010) mutagenesis function (Figures 1B, 2B, rightmost panel, 5, 6, and S1). Contact distances between CFTR ICL1 and ICL4 residues and murine WT or ΔF508 NBD1 residues were calculated via a Perl script using the atomic coordinates from the models.

CFTR Function

The whole-cell patch-clamp technique was used to measure Cl^- current as previously described (Wang et al., 2006). Briefly, whole cell conductance responses were measured in response to 10 μM forskolin + 100 μM IBMX and then 10 μM Inhibitor-172 (Inh-172). Current recording and analysis was performed with pClamp 9.2 software and analyzed with Origin 8 software. Transepithelial conductance (G_t) measurements across monolayers of transiently transfected FRT cells were performed using an EVOM^2 Epithelial Voltohmmeter with a STX100 electrode (World Precision Instruments) at 37°C. G_t was measured 10 minutes after treatment with 10 μM Forskolin + 100 μM IBMX and 5 minutes after 20 μM Inh-172.

Supplementary Material

Refer to Web version on PubMed Central for supplementary material.

Acknowledgments

The authors wish to thank Linda Millen, Bala Somalinga and David Thompson for suggestions and technical assistance, the CFTR Folding Consortium for intellectual support, and the CFF, NIDDK and NDCR for grant support.

References

Accurso FJ, Rowe SM, Clancy JP, Boyle MP, Dunitz JM, Durie PR, Sagel SD, Hornick DB, Konstan MW, Donaldson SH, et al. Effect of VX-770 in persons with cystic fibrosis and the G551D-CFTR mutation. N Engl J Med. 2010; 363:1991–2003. [PubMed: 21083385]

Altschul SF, Madden TL, Schaffer AA, Zhang J, Zhang Z, Miller W, Lipman DJ. Gapped BLAST and PSI-BLAST: a new generation of protein database search programs. Nucleic acids research. 1997; 25:3389–3402. [PubMed: 9254694]

Atwell S, Brouillette CG, Conners K, Emtage S, Gheyi T, Guggino WB, Hendle J, Hunt JF, Lewis HA, Lu F, et al. Structures of a minimal human CFTR first nucleotide-binding domain as a

monomer, head-to-tail homodimer, and pathogenic mutant. Protein Eng Des Sel. 2010; 23:375–384. [PubMed: 20150177]

Berger AL, Ikuma M, Welsh MJ. Normal gating of CFTR requires ATP binding to both nucleotide-binding domains and hydrolysis at the second nucleotide-binding domain. Proc Natl Acad Sci U S A. 2005; 102:455–460. [PubMed: 15623556]

Cheng SH, Gregory RJ, Marshall J, Paul S, Souza DW, White GA, O'Riordan CR, Smith AE. Defective intracellular transport and processing of CFTR is the molecular basis of most cystic fibrosis. Cell. 1990; 63:827–834. [PubMed: 1699669]

Clamp M, Cuff J, Searle SM, Barton GJ. The Jalview Java alignment editor. Bioinformatics. 2004; 20:426–427. [PubMed: 14960472]

Dawson RJ, Locher KP. Structure of the multidrug ABC transporter Sav1866 from Staphylococcus aureus in complex with AMP-PNP. FEBS Lett. 2007; 581:935–938. [PubMed: 17303126]

Dean M, Allikmets R. Evolution of ATP-binding cassette transporter genes. Curr Opin Genet Dev. 1995; 5:779–785. [PubMed: 8745077]

Dean M, Annilo T. Evolution of the ATP-binding cassette (ABC) transporter superfamily in vertebrates. Annu Rev Genomics Hum Genet. 2005; 6:123–142. [PubMed: 16124856]

DeCarvalho AC, Gansheroff LJ, Teem JL. Mutations in the nucleotide binding domain 1 signature motif region rescue processing and functional defects of cystic fibrosis transmembrane conductance regulator delta f508. J Biol Chem. 2002; 277:35896–35905. [PubMed: 12110684]

Dekker JP, Fodor A, Aldrich RW, Yellen G. A perturbation-based method for calculating explicit likelihood of evolutionary co-variance in multiple sequence alignments. Bioinformatics. 2004; 20:1565–1572. [PubMed: 14962924]

Denning GM, Anderson MP, Amara JF, Marshall J, Smith AE, Welsh MJ. Processing of mutant cystic fibrosis transmembrane conductance regulator is temperature-sensitive. Nature. 1992; 358:761–764. [PubMed: 1380673]

Dork T, Wulbrand U, Richter T, Neumann T, Wolfes H, Wulf B, Maass G, Tummler B. Cystic fibrosis with three mutations in the cystic fibrosis transmembrane conductance regulator gene. Hum Genet. 1991; 87:441–446. [PubMed: 1715308]

Du K, Sharma M, Lukacs GL. The DeltaF508 cystic fibrosis mutation impairs domain-domain interactions and arrests post-translational folding of CFTR. Nat Struct Mol Biol. 2005; 12:17–25. [PubMed: 15619635]

Fodor AA, Aldrich RW. Influence of conservation on calculations of amino acid covariance in multiple sequence alignments. Proteins. 2004; 56:211–221. [PubMed: 15211506]

Goh CS, Bogan AA, Joachimiak M, Walther D, Cohen FE. Co-evolution of proteins with their interaction partners. J Mol Biol. 2000; 299:283–293. [PubMed: 10860738]

Hoelen H, Kleizen B, Schmidt A, Richardson J, Charitou P, Thomas PJ, Braakman I. The primary folding defect and rescue of DeltaF508 CFTR emerge during translation of the mutant domain. PLoS One. 2010; 5:e15458. [PubMed: 21152102]

Jones PM, George AM. The ABC transporter structure and mechanism: perspectives on recent research. Cell Mol Life Sci. 2004; 61:682–699. [PubMed: 15052411]

Kass I, Horovitz A. Mapping pathways of allosteric communication in GroEL by analysis of correlated mutations. Proteins. 2002; 48:611–617. [PubMed: 12211028]

Krasnov KV, Tzetis M, Cheng J, Guggino WB, Cutting GR. Localization studies of rare missense mutations in cystic fibrosis transmembrane conductance regulator (CFTR) facilitate interpretation of genotype-phenotype relationships. Hum Mutat. 2008; 29:1364–1372. [PubMed: 18951463]

Kunichika K, Hashimoto Y, Imoto T. Robustness of hen lysozyme monitored by random mutations. Protein Eng. 2002; 15:805–809. [PubMed: 12468714]

Larkin MA, Blackshields G, Brown NP, Chenna R, McGettigan PA, McWilliam H, Valentin F, Wallace IM, Wilm A, Lopez R, et al. Clustal W and Clustal X version 2.0. Bioinformatics. 2007; 23:2947–2948. [PubMed: 17846036]

Lewis HA, Buchanan SG, Burley SK, Conners K, Dickey M, Dorwart M, Fowler R, Gao X, Guggino WB, Hendrickson WA, et al. Structure of nucleotide-binding domain 1 of the cystic fibrosis transmembrane conductance regulator. Embo J. 2004; 23:282–293. [PubMed: 14685259]

Lewis HA, Wang C, Zhao X, Hamuro Y, Conners K, Kearins MC, Lu F, Sauder JM, Molnar KS, Coales SJ, et al. Structure and dynamics of NBD1 from CFTR characterized using crystallography and hydrogen/deuterium exchange mass spectrometry. J Mol Biol. 2010; 396:406–430. [PubMed: 19944699]

Lewis HA, Zhao X, Wang C, Sauder JM, Rooney I, Noland BW, Lorimer D, Kearins MC, Conners K, Condon B, et al. Impact of the deltaF508 mutation in first nucleotide-binding domain of human cystic fibrosis transmembrane conductance regulator on domain folding and structure. J Biol Chem. 2005; 280:1346–1353. [PubMed: 15528182]

Lockless SW, Ranganathan R. Evolutionarily conserved pathways of energetic connectivity in protein families. Science. 1999; 286:295–299. [PubMed: 10514373]

Madaoui H, Guerois R. Coevolution at protein complex interfaces can be detected by the complementarity trace with important impact for predictive docking. Proc Natl Acad Sci U S A. 2008; 105:7708–7713. [PubMed: 18511568]

McCarty NA. Permeation through the CFTR chloride channel. J Exp Biol. 2000; 203:1947–1962. [PubMed: 10851114]

Mendoza JL, Thomas PJ. Building an understanding of cystic fibrosis on the foundation of ABC transporter structures. J Bioenerg Biomembr. 2007; 39:499–505. [PubMed: 18080175]

Pazos F, Valencia A. Protein co-evolution, co-adaptation and interactions. Embo J. 2008; 27:2648–2655. [PubMed: 18818697]

Pedemonte N, Lukacs GL, Du K, Caci E, Zegarra-Moran O, Galietta LJ, Verkman AS. Small-molecule correctors of defective DeltaF508-CFTR cellular processing identified by high-throughput screening. J Clin Invest. 2005; 115:2564–2571. [PubMed: 16127463]

Pei J, Grishin NV. AL2CO: calculation of positional conservation in a protein sequence alignment. Bioinformatics. 2001; 17:700–712. [PubMed: 11524371]

Pei J, Kim BH, Grishin NV. PROMALS3D: a tool for multiple protein sequence and structure alignments. Nucleic acids research. 2008a; 36:2295–2300. [PubMed: 18287115]

Pei J, Tang M, Grishin NV. PROMALS3D web server for accurate multiple protein sequence and structure alignments. Nucleic acids research. 2008b; 36:W30–34. [PubMed: 18503087]

Pissarra LS, Farinha CM, Xu Z, Schmidt A, Thibodeau PH, Cai Z, Thomas PJ, Sheppard DN, Amaral MD. Solubilizing mutations used to crystallize one CFTR domain attenuate the trafficking and channel defects caused by the major cystic fibrosis mutation. Chem Biol. 2008; 15:62–69. [PubMed: 18215773]

Pjura P, Matsumura M, Baase WA, Matthews BW. Development of an in vivo method to identify mutants of phage T4 lysozyme of enhanced thermostability. Protein Sci. 1993; 2:2217–2225. [PubMed: 7507755]

Protasevich I, Yang Z, Wang C, Atwell S, Zhao X, Emtage S, Wetmore D, Hunt JF, Brouillette CG. Thermal unfolding studies show the disease causing F508del mutation in CFTR thermodynamically destabilizes nucleotide-binding domain 1. Protein Sci. 2010; 19:1917–1931. [PubMed: 20687133]

Qu BH, Strickland EH, Thomas PJ. Localization and suppression of a kinetic defect in cystic fibrosis transmembrane conductance regulator folding. J Biol Chem. 1997; 272:15739–15744. [PubMed: 9188468]

Qu BH, Thomas PJ. Alteration of the cystic fibrosis transmembrane conductance regulator folding pathway. J Biol Chem. 1996; 271:7261–7264. [PubMed: 8631737]

Rich DP, Anderson MP, Gregory RJ, Cheng SH, Paul S, Jefferson DM, McCann JD, Klinger KW, Smith AE, Welsh MJ. Expression of cystic fibrosis transmembrane conductance regulator corrects defective chloride channel regulation in cystic fibrosis airway epithelial cells. Nature. 1990; 347:358–363. [PubMed: 1699126]

Riordan JR, Rommens JM, Kerem B, Alon N, Rozmahel R, Grzelczak Z, Zielenski J, Lok S, Plavsic N, Chou JL, et al. Identification of the cystic fibrosis gene: cloning and characterization of complementary DNA. Science. 1989; 245:1066–1073. [PubMed: 2475911]

Robert R, Carlile GW, Liao J, Balghi H, Lesimple P, Liu N, Kus B, Rotin D, Wilke M, de Jonge HR, et al. Correction of the Delta phe508 cystic fibrosis transmembrane conductance regulator

trafficking defect by the bioavailable compound glafenine. Mol Pharmacol. 2010; 77:922–930. [PubMed: 20200141]

Robert R, Carlile GW, Pavel C, Liu N, Anjos SM, Liao J, Luo Y, Zhang D, Thomas DY, Hanrahan JW. Structural analog of sildenafil identified as a novel corrector of the F508del-CFTR trafficking defect. Mol Pharmacol. 2008; 73:478–489. [PubMed: 17975008]

Roxo-Rosa M, Xu Z, Schmidt A, Neto M, Cai Z, Soares CM, Sheppard DN, Amaral MD. Revertant mutants G550E and 4RK rescue cystic fibrosis mutants in the first nucleotide-binding domain of CFTR by different mechanisms. Proc Natl Acad Sci U S A. 2006; 103:17891–17896. [PubMed: 17098864]

Sampson HM, Robert R, Liao J, Matthes E, Carlile GW, Hanrahan JW, Thomas DY. Identification of a NBD1-binding pharmacological chaperone that corrects the trafficking defect of F508del-CFTR. Chem Biol. 2011; 18:231–242. [PubMed: 21338920]

Schrodinger LLC. The PyMOL Molecular Graphics System, Version 1.3r1. 2010

Socolich M, Lockless SW, Russ WP, Lee H, Gardner KH, Ranganathan R. Evolutionary information for specifying a protein fold. Nature. 2005; 437:512–518. [PubMed: 16177782]

Stratford FL, Ramjeesingh M, Cheung JC, Huan LJ, Bear CE. The Walker B motif of the second nucleotide-binding domain (NBD2) of CFTR plays a key role in ATPase activity by the NBD1-NBD2 heterodimer. Biochem J. 2007; 401:581–586. [PubMed: 16989640]

Teem JL, Berger HA, Ostedgaard LS, Rich DP, Tsui LC, Welsh MJ. Identification of revertants for the cystic fibrosis delta F508 mutation using STE6-CFTR chimeras in yeast. Cell. 1993; 73:335–346. [PubMed: 7682896]

Teem JL, Carson MR, Welsh MJ. Mutation of R555 in CFTR-delta F508 enhances function and partially corrects defective processing. Receptors Channels. 1996; 4:63–72. [PubMed: 8723647]

Thibodeau PH, Brautigam CA, Machius M, Thomas PJ. Side chain and backbone contributions of Phe508 to CFTR folding. Nat Struct Mol Biol. 2005; 12:10–16. [PubMed: 15619636]

Thibodeau PH, Richardson JM 3rd, Wang W, Millen L, Watson J, Mendoza JL, Du K, Fischman S, Senderowitz H, Lukacs GL, et al. The cystic fibrosis-causing mutation deltaF508 affects multiple steps in cystic fibrosis transmembrane conductance regulator biogenesis. J Biol Chem. 2010; 285:35825–35835. [PubMed: 20667826]

Thomas PJ, Shenbagamurthi P, Sondek J, Hullihen JM, Pedersen PL. The cystic fibrosis transmembrane conductance regulator. Effects of the most common cystic fibrosis-causing mutation on the secondary structure and stability of a synthetic peptide. J Biol Chem. 1992; 267:5727–5730. [PubMed: 1372891]

Van Goor F, Hadida S, Grootenhuis PD, Burton B, Cao D, Neuberger T, Turnbull A, Singh A, Joubran J, Hazlewood A, et al. Rescue of CF airway epithelial cell function in vitro by a CFTR potentiator, VX-770. Proc Natl Acad Sci U S A. 2009; 106:18825–18830. [PubMed: 19846789]

Van Goor F, Hadida S, Grootenhuis PD, Burton B, Stack JH, Straley KS, Decker CJ, Miller M, McCartney J, Olson ER, et al. Correction of the F508del-CFTR protein processing defect in vitro by the investigational drug VX-809. Proc Natl Acad Sci U S A. 2011

Van Goor F, Straley KS, Cao D, Gonzalez J, Hadida S, Hazlewood A, Joubran J, Knapp T, Makings LR, Miller M, et al. Rescue of DeltaF508-CFTR trafficking and gating in human cystic fibrosis airway primary cultures by small molecules. Am J Physiol Lung Cell Mol Physiol. 2006; 290:L1117–1130. [PubMed: 16443646]

Vergani P, Lockless SW, Nairn AC, Gadsby DC. CFTR channel opening by ATP-driven tight dimerization of its nucleotide-binding domains. Nature. 2005; 433:876–880. [PubMed: 15729345]

Vergani P, Nairn AC, Gadsby DC. On the mechanism of MgATP-dependent gating of CFTR Cl- channels. J Gen Physiol. 2003; 121:17–36. [PubMed: 12508051]

Walker JE, Saraste M, Runswick MJ, Gay NJ. Distantly related sequences in the alpha- and beta-subunits of ATP synthase, myosin, kinases and other ATP-requiring enzymes and a common nucleotide binding fold. Embo J. 1982; 1:945–951. [PubMed: 6329717]

Wang C, Protasevich I, Yang Z, Seehausen D, Skalak T, Zhao X, Atwell S, Spencer Emtage J, Wetmore DR, Brouillette CG, et al. Integrated biophysical studies implicate partial unfolding of NBD1 of CFTR in the molecular pathogenesis of F508del cystic fibrosis. Protein Sci. 2010; 19:1932–1947. [PubMed: 20687163]

Wang Y, Soyombo AA, Shcheynikov N, Zeng W, Dorwart M, Marino CR, Thomas PJ, Muallem S. Slc26a6 regulates CFTR activity in vivo to determine pancreatic duct HCO3- secretion: relevance to cystic fibrosis. Embo J. 2006; 25:5049–5057. [PubMed: 17053783]

Waterhouse AM, Procter JB, Martin DM, Clamp M, Barton GJ. Jalview Version 2--a multiple sequence alignment editor and analysis workbench. Bioinformatics. 2009; 25:1189–1191. [PubMed: 19151095]

Wigley WC, Stidham RD, Smith NM, Hunt JF, Thomas PJ. Protein solubility and folding monitored in vivo by structural complementation of a genetic marker protein. Nat Biotechnol. 2001; 19:131–136. [PubMed: 11175726]

Highlights

- Statistical coupling analyses reveal positions linked to F508
- Coupled positions reveal the ΔF508 mutation interferes with two steps in CFTR folding
- Two defects of ΔF508 misfolding explain the efficacy ceiling observed for correctors
- Correction of both defective steps is synergistic and required to restore function

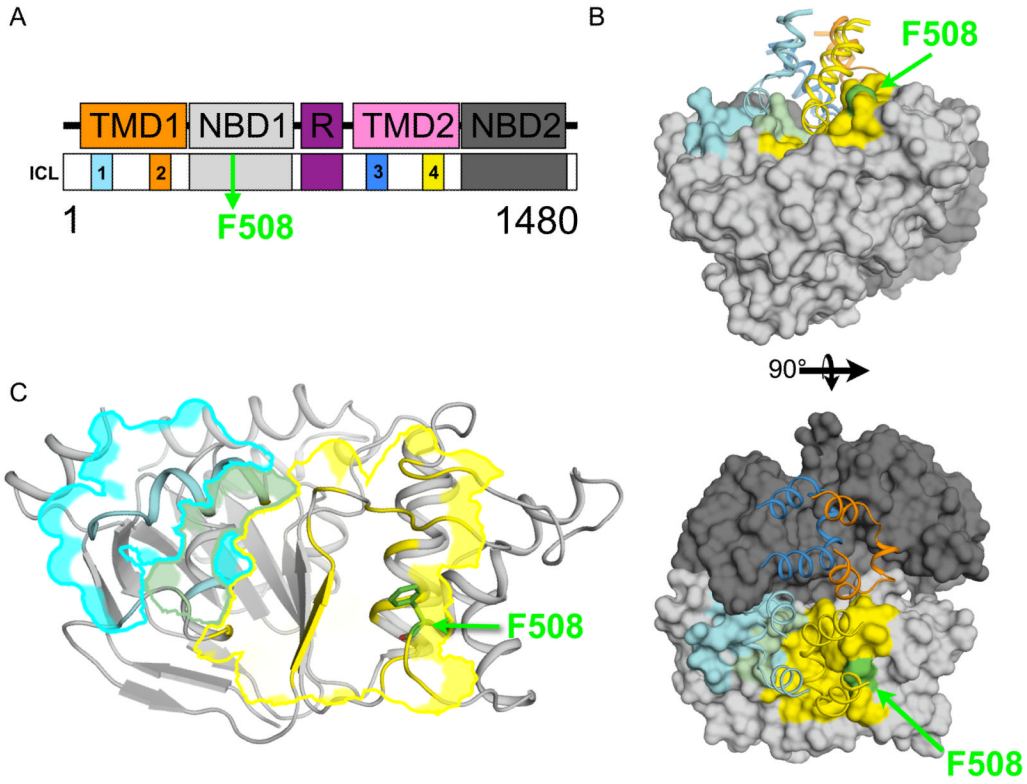

Figure 1. Relationship of CFTR Domains to the F508 Position

(**A**) CFTR is 1480 amino acids in length and contains two transmembrane domains (TMDs, orange and pink) and four intracellular loops (labeled ICL1–4, cyan, orange, blue, and yellow), two nucleotide binding domains (NBDs, grey and charcoal) and a highly disordered Regulatory region (R, purple). F508, green is located within the NBD1 domain. (**B**) The Sav1866 based homology model of CFTR *sans* R-region (pdbs 2HYD, 1R0W, and 3GD7). (*top*) View of the NBDs and ICLs of CFTR parallel to the membrane. The two NBDs associate in a head-to-tail fashion. ICL1 (cyan ribbon) and ICL4 (yellow ribbon) interact with NBD1 and ICL2 (orange ribbon) and ICL3 (blue ribbon) interact with NBD2. F508 (green surface) is at the predicted interface with ICL4. NBD1 surface residues predicted to be within 6 Å of ICL1, ICL4 or both are highlighted in cyan, yellow or light green respectively. (*bottom*) View of the CFTR model looking down from the membrane (90° relative to top). See also Figure S1. (**C**) Ribbon representation of NBD1 (pdb 1R0W) showing relationship of F508 (green sticks) to the predicted interface with ICL4 yellow outline.

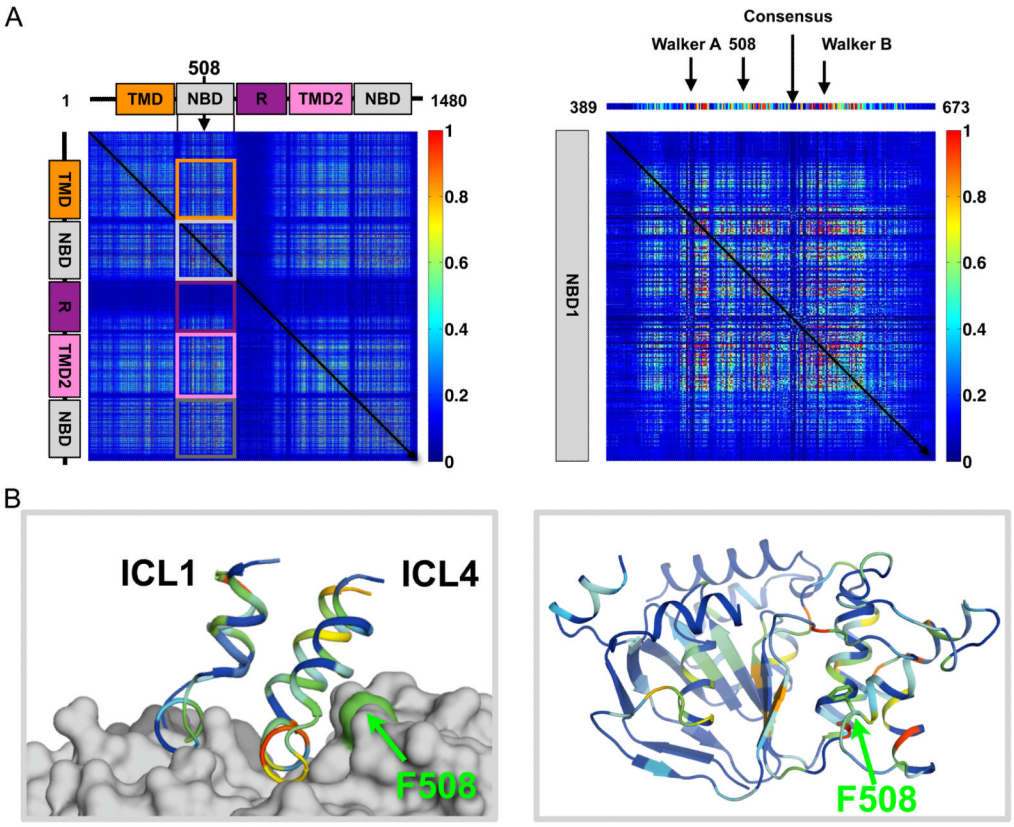

Figure 2. CFTR Inter-Residue Coupling Matrix Calculated from an ABC Transporter Sequence Alignment

(**A**) (*left*) Heat map of the 1480 × 1480 matrix representing a linear combination of statistical methods (SCA, ELSC, OMES, McBASC). The color scale (*right*) with statistical scores approaching zero represented by dark blue and scores of high statistical significance in red. The diagonal denotes identity. Coupling of each of the five domains of CFTR to NBD1 are shown in squares with TMD1 in orange, NBD1 coupling to itself in light gray, the R-region in purple, TMD2 in pink, and NBD2 in dark gray. See also Figure S2. (*right*) The 285 × 285 matrix of coupling scores within NBD1 (positions 389 to 673 of the left panel). Above the matrix is the column of coupling scores for every position in NBD1 to the 508 position. The conserved Walker A and B, Consensus motifs, and the 508 position are denoted by arrows. (**B**) (*left*) The 508-coupling scores in ICL1 (residues 158-184) and ICL4 (residues 1050-1080) of the CFTR model (Figure 1B). The surface corresponding to the F508 position is colored in green and is predicted to be in contact with ICL4. (*right*) View of NBD1 (pdb 1R0W) colored with normalized scores from panel C. The F508 position is shown in green.

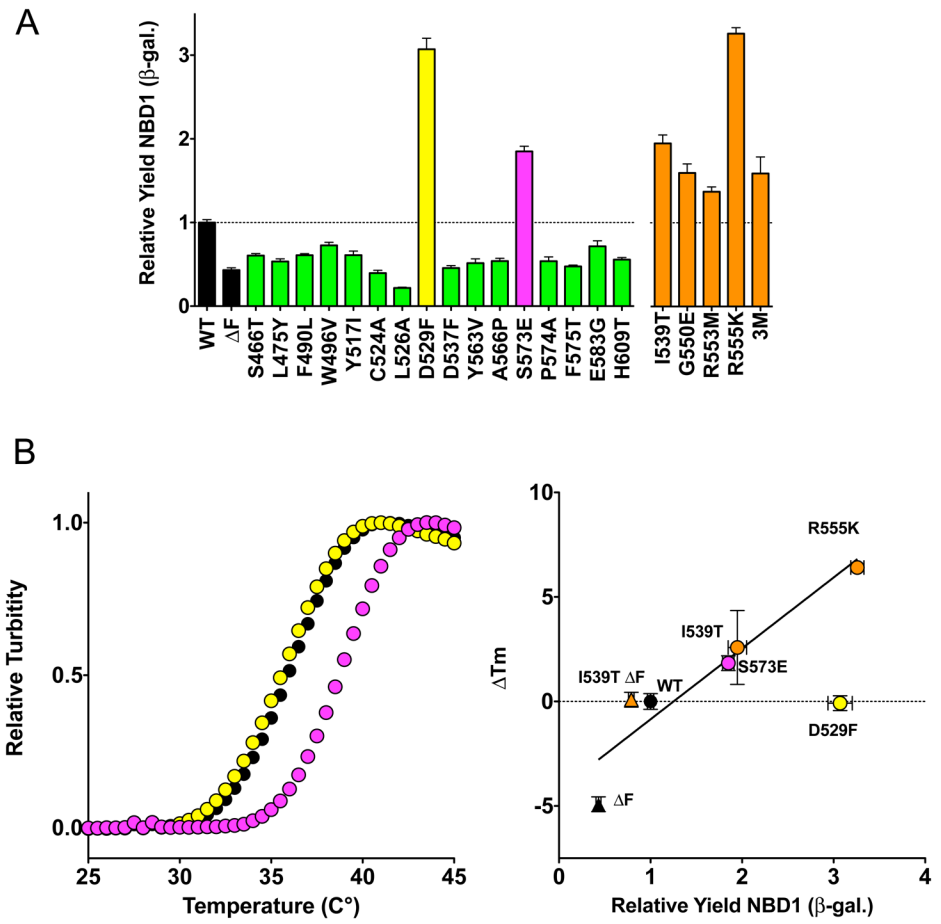

Figure 3. Effects of 508-Coupled Mutations and Second-Site Suppressors on NBD1 Folding

(**A**) The relative yield of NBD1 folding was determined using a cell-based assay. All mutations altered the relative yield relative to wild type NBD1 as shown in the bar chart (+/−SEM, n=9 except for WT, ΔF508, D529F, and S573E where n=18). Two of the 508-coupled positions, D529F and S573E, increase the yield of NBD1. The remaining mutations decrease the yield of soluble NBD1. (**B**) (top panel) Thermal denaturation of 5 μM purified recombinant WT, D529F, and S573E NBD1 in the presence of 2 mM ATP. See also Figure S4. By contrast to the increased NBD1 folding yield, the D529F mutation (yellow circles) has no observable effect on thermal stability relative to WT (black circles). S573E (magenta circles) increased the melting temperature 2° C. (lower panel) Correlation between thermal stability of bacterially expressed and purified NBD1 and NBD1 folding yield. For mutants on either WT (circles) or ΔF (triangles) backgrounds, the correlation between stability and folding yield, R = 0.94 when D529F is excluded (yellow circle).

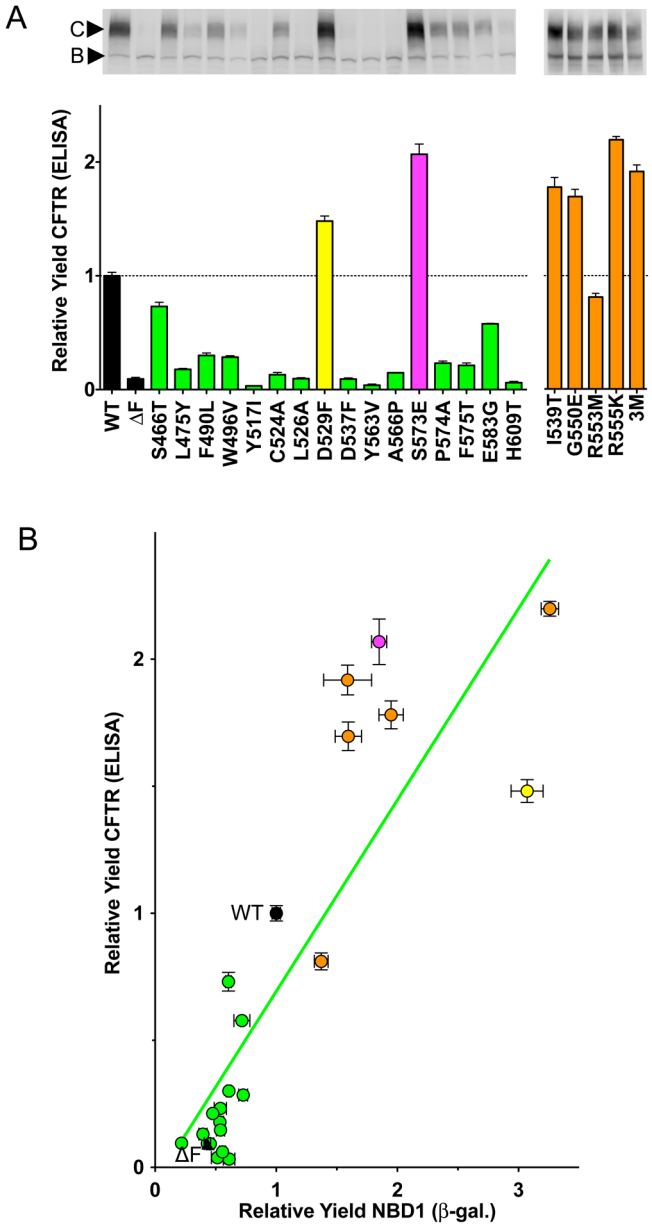

Figure 4. Effects of 508-Coupled and Second-Site Suppressor Mutations on CFTR Maturation: Correlation with NBD1 Folding Yield

Effects of 508-coupled mutations (green, yellow, and magenta) and second-site suppressors (orange) on the maturation of full-length CFTR and correlation with NBD1 folding yield. (**A**) The efficiency of full-length CFTR maturation was determined by ELISA (+/− SEM, n=6 for WT, ΔF508, D529F, and S573E, n=3 for other mutants). A control western blot is shown above the bar graph. All mutations altered maturation relative to wild type CFTR. The two 508-coupled positions that increased NBD1 folding yield, D529F and S573E, also increased the maturation yield of CFTR (yellow and magenta bars, respectively). See also Figure S5. (**B**) The influence of the 508-coupled mutations (green circles), four second-site suppressor mutations (I539T, G550E, R553M, and R555K) and three suppressors in combination (G550E, R553M, and R555K) (orange circles) on F508 background on relative maturation of full-length CFTR and relative NBD1 folding yield is correlated (green line, m

= 0.75, R = 0.85). The two F508 coupled position mutations, D529F and S573E, are colored in yellow and magenta circles, respectively.

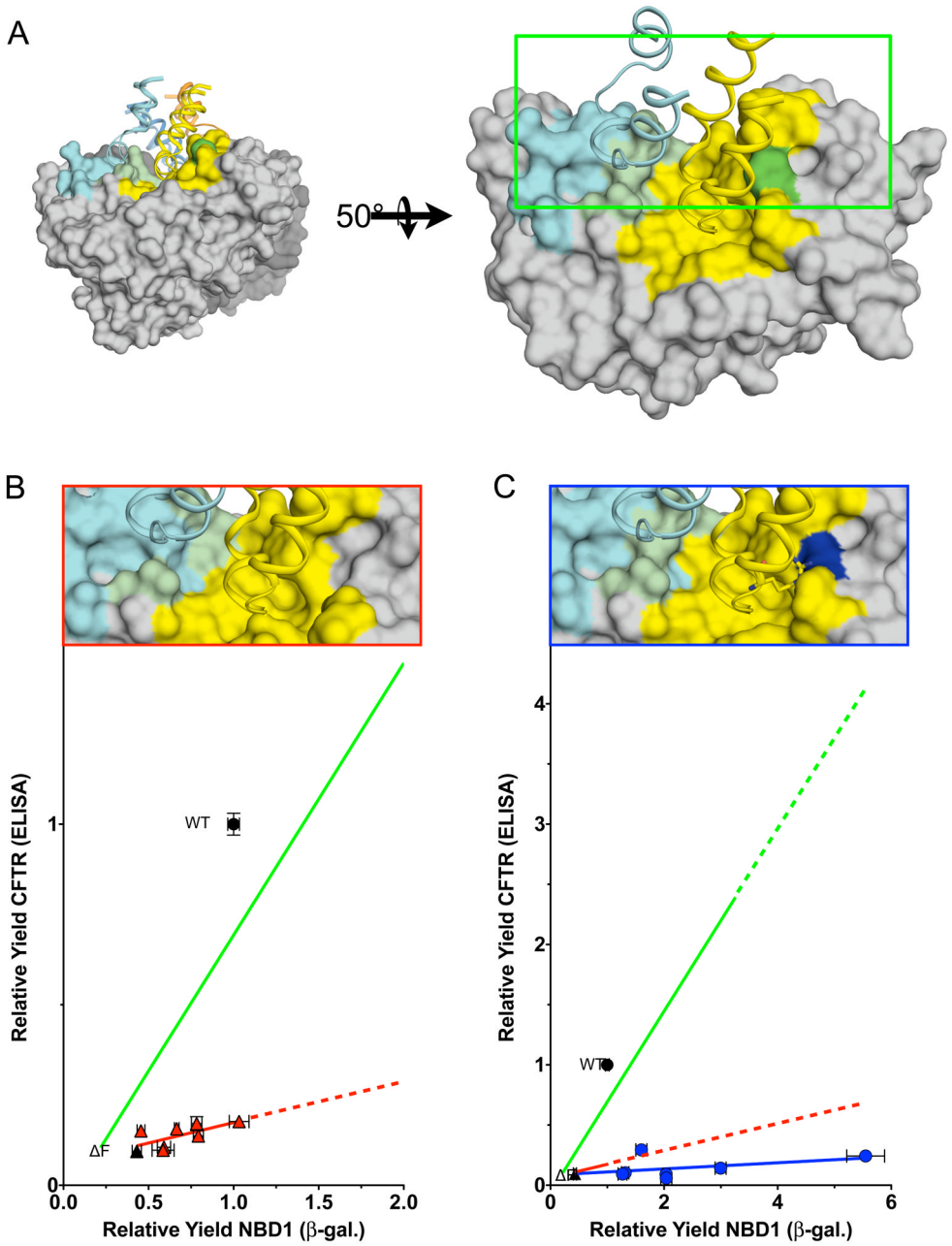

Figure 5. ΔF508 and 508 Missense Mutations Influence the Correlation of CFTR Maturation with NBD1 Folding Yield

(**A**) View of the CFTR NBD1 ICL1/4 interface, as described in Figure 1B. (**B**) Deletion of the F508 residue creates a pocket on the NBD1 surface near the predicted ICL4 interface (compare ΔF508 Figure 5B, pdb 3SI7, to wild type Figure 1C, pdb 1R0W). See also Table S1. Previously identified second-site suppressor (I539T, G550E, R553M, R555K, and 3M) but not the 508-coupled mutants (D529F and S573E), increase the yield of ΔF508 NBD1. The correlation between increased NBD1 yield and relative yield of ΔF508 CFTR is shallower (red line, m = 0.10, R = 0.36) than wild type (green line, m = 0.75, R = 0.85). See also Table S2. (**C**) F508K, F508R, and F508K in combination with I539T, G550E, R553M, R555K, and 3M mutations increase folding yield of NBD1, but exhibit no corresponding increase in CFTR maturation yield (dark blue circles and line, m = 0.03, R = 0.40).

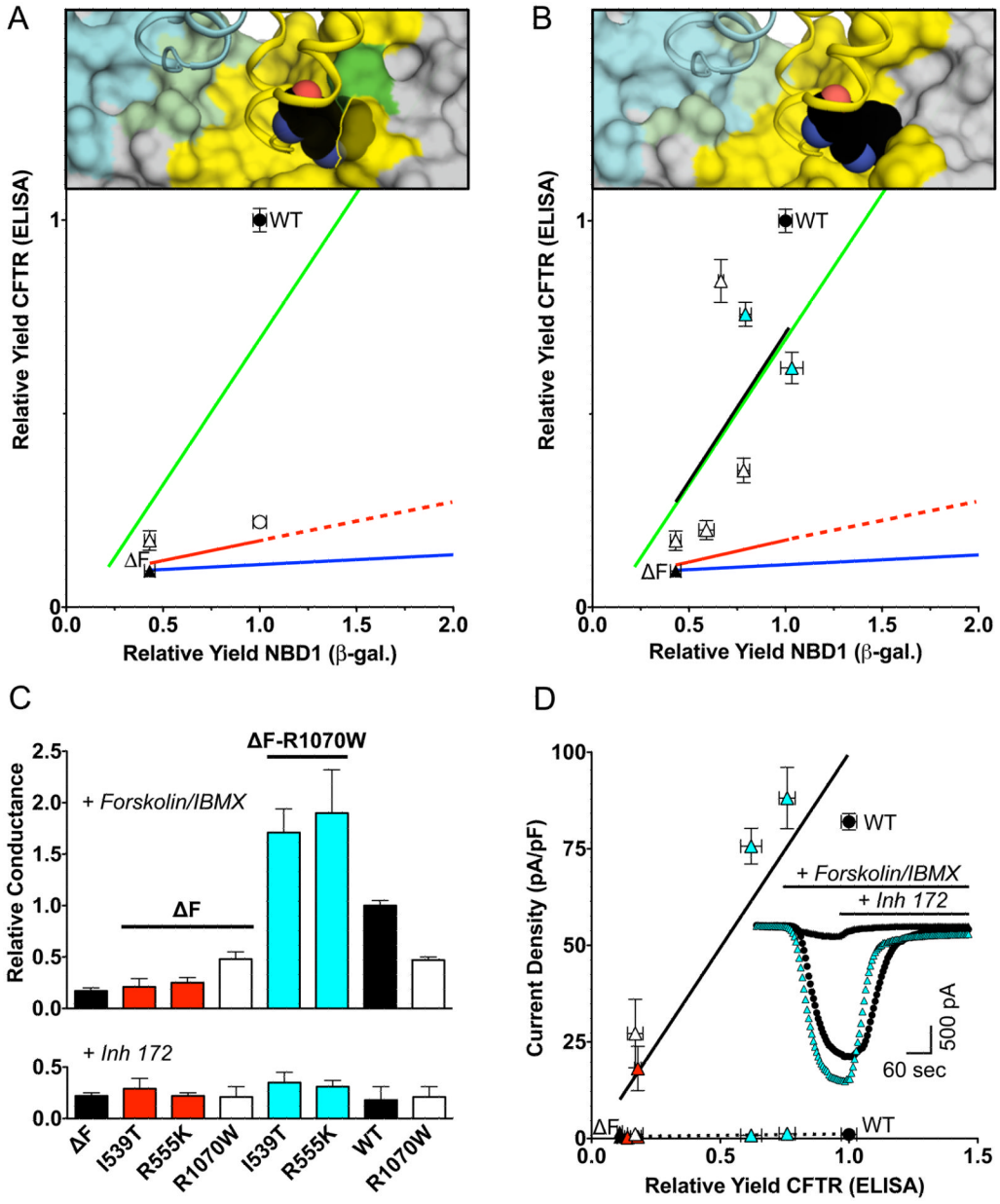

Figure 6. Correction of the ΔF508 NBD1/ICL4 Interface Defect is Synergistic with Correction of the ΔF508 NBD1 Folding Yield Defect

(A) CFTR maturation yield as a function of NBD1 folding yield for wild type, ΔF508, and the ICL4/NBD1 interface mutants are shown as green, red and dark blue lines for comparison. The R1070W (open triangle) mutation in ICL4 modestly improves the relative yield of ΔF508 CFTR maturation and decreases the relative yield for CFTR wild type (open circle) consistent with he predicted steric clash with the F508 side-chain (*top*). **(B)** By contrast, in the model Trp is accommodated by the pocket formed by the ΔF508 mutant (pdb 3SI7) See also Table S1. (*top*). When R1070W is combined with mutations that improve ΔF508 NBD1 folding yield, I539T, G550E, R553M, R555K, and 3M (open triangles), the correlation between NBD1 folding and CFTR maturation in the wild type protein is restored (m = 0.77, R = 0.47, black line). See also Table S2. **(C)** CFTR-dependent transepithelial conductance. Monolayers of FRT cells transiently expressing CFTR were stimulated with

10μM Forskolin + 100μM IBMX and transepithelial conductance measured (*top*, +/−SEM, n=3, average conductance for wild type = 1.24 mS). The CFTR dependence of conductance is indicated by the sensitivity to 20 μM Inh-172 (*bottom*). See also Table S2. **(D)** Forskolin stimulated, Inh-172 sensitive whole cell currents of HeLa cells transiently expressing CFTR reveal a correlation between Current Density after activation (10 μM forskolin + 100 μM IBMX) with relative yield of CFTR (black line, +/−SEM, n = 5–6) and in the presence of Inh-172 (10 μM) dotted line (+/−SEM, n=4–6). A representative trace of the corrected mutant, ΔF508-I539T-R1070W CFTR (cyan triangles) is more like wild type (filled circles) than ΔF508 (filled triangles) (*inset*). See also Table S2.

Table 1

NBD1 Positions Coupled to F508

The alignment of 493 sequences was used to calculate pairwise coupling scores using each method (ELSC, SCA, McBASC, and OMES). The top twenty are shown for each method, the top ten positions in bold. The tested set of 16 positions are underlined. See also Figure S3.

ELSC	McBASC	OMES	SCA
			435
		453	
		460	
		S466T	**S466T**
	468		
		470	
	472		
		473	473
		474	474
L475Y		L475Y	L475Y
	F490L		**F490L**
W496V	**W496V**	W496V	**W496V**
	503		
	505		
	507		
	509		
512			
513			
Y517I	**Y517I**	**Y517I**	**Y517I**
		520	520
	521		
C524A	C524A	**C524A**	**C524A**
L526A	**L526A**	**L526A**	**L526A**
D529F	**D529F**	**D529F**	**D529F**
D537F			**D537F**
	543		
Y563V	**Y563V**	Y563V	**Y563V**
A566P		A566P	
		569	569
			S573E
P574A		**P574A**	P574A
F575T		**F575T**	
			578
582			
E583G		E583G	
587			
	591		

ELSC	McBASC	OMES	SCA
	595		
	598		
	602		
604		**604**	**604**
H609T			
	617		
630			630
640			